
MoE-CAP: Cost-Accuracy-Performance Benchmarking for Mixture-of-Experts Systems

Yao Fu^{*1}, Yinsicheng Jiang^{*1}, Yeqi Huang^{*1}, Ping Nie³, Zhan Lu¹, Leyang Xue¹, Congjie He¹,
Man-Kit Sit¹, Jilong Xue², Li Dong², Ziming Miao², Kai Zou⁴, Edoardo Ponti¹, Luo Mai¹

¹University of Edinburgh, ²Microsoft Research, ³Peking University, ⁴NetMind.AI

Abstract

The sparse Mixture-of-Experts (MoE) architecture is increasingly favored for scaling Large Language Models (LLMs) efficiently; however, MoE systems rely on heterogeneous compute and memory resources. These factors collectively influence the system’s Cost, Accuracy, and Performance (CAP), creating a challenging trade-off. Current benchmarks often fail to provide precise estimates of these effects, complicating practical considerations for deploying MoE systems. To bridge this gap, we introduce MoE-CAP, a benchmark specifically designed to evaluate MoE systems. Our findings highlight the difficulty of achieving an optimal balance of cost, accuracy, and performance with existing hardware capabilities. MoE systems often necessitate compromises on one factor to optimize the other two, a dynamic we term the MoE-CAP trade-off. To identify the best trade-off, we propose novel performance evaluation metrics—Sparse Memory Bandwidth Utilization (S-MBU) and Sparse Model FLOPS Utilization (S-MFU)—and develop cost models that account for the heterogeneous compute and memory hardware integral to MoE systems. This benchmark is publicly available on HuggingFace: <https://huggingface.co/spaces/sparse-generative-ai/open-moe-1lm-leaderboard>.

1 Introduction

Recent large language models (LLMs) are increasingly adopting sparse Mixture-of-Experts (MoE) architectures, notable examples of which include Switch-C (Fedus et al., 2022), DBRX, Mixtral-8x22B (Jiang et al., 2024), Snowflake Arctic (Snowflake AI Research, 2024), Grok-1 (XAI, 2024), DeepSeek-MoE (Dai et al., 2024), and Qwen1.5-MoE (Bai et al., 2023). These models utilize sparse experts grouped into an MoE layer, and these experts are selectively activated through a router (or a gating network). By routing tokens to a subset of experts, MoEs achieve sub-linear computational costs compared to their dense equivalents, which allows building trillion-parameter-scale LLMs.

Current MoE systems exhibit increasing complexity, driven by two main factors: (i) There is enhanced sophistication in the design of sparse MoE layers and gating networks (or routers), which differ in sparsity characteristics across various MoE models; (ii) MoEs demonstrate sub-linear computational complexity, enabling the offloading of less frequently activated experts onto external memory and processors. This approach reduces dependence on costly High Bandwidth Memory (HBM) on GPUs. Consequently, the complexity of servers hosting MoE systems has escalated, with these servers typically featuring heterogeneous compute, memory, and communication resources, arranged in a multi-tier architecture. For instance, modern MoE systems increasingly offload experts to DRAM and SSDs (Xue et al., 2024, Eliseev and Mazur, 2023) and delegate part of the computation to CPUs (Kamahori et al., 2024).

*Equal contribution.

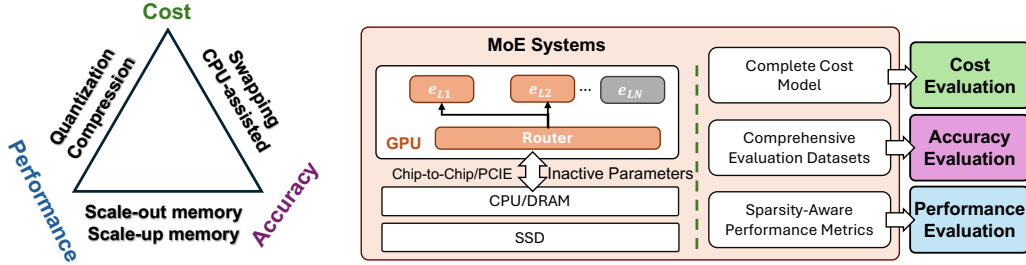


Figure 1: Overview of MoE-CAP. **Left:** We identify trade-offs between Cost, Accuracy, and Performance (corners) driven by design and deployment choices (sides). **Right:** MoE-CAP contributions include new sparsity-aware metrics for performance, accuracy evaluation on diverse tasks, and a complete deployment cost model for MoE systems.

Practitioners of MoE systems are actively seeking methods to benchmark their cost, accuracy (in downstream tasks), and performance (time and memory efficiency) in order to optimize their deployment. However, this benchmarking is challenging for the following reasons: (i) *Poor understanding of the relation between cost, accuracy and performance:* MoE systems often claim advantages in cost, accuracy, and performance, but real-world deployments frequently reveal underestimated costs, under-achievements in performance benefits, and compromised accuracy. Clear principles are needed to help practitioners effectively evaluate and understand the complex interplay between these factors, (ii) *Inadequate system performance assessment metrics:* Existing metrics like Memory Bandwidth Utilization (MBU; Agarwal et al., 2023) and Model FLOPS Utilization (MFU; Chowdhery et al., 2023) are tailored for dense LLMs and fail to account for the sparse activation patterns of experts in MoE systems. This oversight leads to overestimated memory and compute costs, resulting in inefficient use of over-provisioned GPU resources, (iii) *Incomplete system deployment cost estimation:* Current benchmarks predominantly estimate costs based on GPU usage alone. However, modern MoE systems increasingly rely on heterogeneous processors (e.g., using CPUs to cover part of MoE computation) and multi-tier memory for parameter swapping (Xue et al., 2024). Ignoring these factors yields inaccurate cost estimations.

To address the above issues, this paper introduces MoE-CAP, a benchmark designed to evaluate and understand the cost, accuracy, and performance of MoE systems. The design of MoE-CAP (illustrated in Figure 1) offers several key contributions:

(1) A method for understanding the trade-off of MoE systems . We analyze a wide range of existing MoE systems and observe that, while these systems often claim to jointly optimize for cost, accuracy, and performance, they in fact can achieve only two of these three properties (cost efficiency, high accuracy, or high performance). This trade-off is fundamentally linked to the router-based, sparse architecture of MoE models and the current hardware capabilities. To facilitate the analysis of this trade-off, we propose a trade-off benchmarking method called CAP.

(2) Sparsity-aware system performance metrics. To enable precise performance assessment of current and future MoE systems, we introduce sparsity-aware performance metrics: Sparse Memory Bandwidth Utilization (Sparse MBU) and Sparse Model FLOPS Utilization (Sparse MFU). These metrics complement existing LLM performance measures, such as prefilling time, first-token latency, and token throughput. By incorporating sparsity into performance evaluation, these metrics help MoE users identify performance bottlenecks and guide the design of improved models and systems.

(3) Complete deployment cost models for MoE systems. We propose cost models that account for the heterogeneous computation resources and multi-tier memory architectures employed in modern MoE systems. These models enable precise estimation of the costs associated with distributing experts across different memory tiers (e.g., on-chip SRAM, on-chip DRAM, and off-chip DRAM, as found in NVIDIA Grace-Hopper 200) and augmenting GPUs with additional CPUs. The models generate practical metrics, such as tokens-per-dollar and tokens-per-kilowatt, which reflect the financial cost and energy efficiency of an MoE system, providing actionable insights for system design and deployment.

Table 1: Characteristics of recent open-source MoE models.

Model	Total Param	Active Param	# of Experts	Top-k + Shared
Switch-C	1571B	12B	128	1
DBRX	132B	36B	16	4
Mistral-8x22B	141B	39B	8	2
Snowflake Arctic	480B	17B	128	2
Grok-1	314B	77B	8	2
DeepSeekMoE	16.4B	2.8B	64	6 + 2
Qwen1.5-MoE	14.3B	2.7B	60	4 + 4

2 Background and Motivation

Sparse MoE models. Many sparse MoE models have been designed recently, and their characteristics are summarized in Table 1. These models typically possess a large number of parameters, with some reaching as high as 1571 billion. During token processing, only a subset of these parameters, generally between 1–25%, is activated. MoE models display diverse sparsity characteristics. For instance, Mistral-8x22B features large experts, each containing 0.3 billion parameters, but restricts the number of experts per layer to just 8. In contrast, Snowflake Arctic uses a much higher number of experts per layer (128), though each expert is smaller, containing only 0.15 billion parameters. The complexity extends to the router design, which typically selects the top-K experts (where K usually ranges from 1 to 4) for activation. Some models also employ a hybrid approach, incorporating a set of always-activated “shared” experts along with a selectively activated group of K experts. These shared experts may differ in size from the selectively activated ones, adding another layer of complexity to the model architecture.

Emerging MoE system designs. MoE systems exhibit sub-linear computational complexity but still require increased memory to accommodate all potentially activated experts. To enhance memory efficiency, several system designs have been explored recently: (i) Designs applying quantization to experts, such as unified quantization for all experts—e.g., GPTQ (Frantar et al., 2022), AWQ (Lin et al., 2023), and SmoothQuant (Xiao et al., 2023)—and expert-specific adaptive quantization—e.g., QMoE (Frantar and Alistarh, 2023) and MoQE (Kim et al., 2023). (ii) Designs offloading experts to external memory. Examples include MoE-layer-wise parameter offloading—e.g., DeepSpeed-Inference (Aminabadi et al., 2022) and SwapAdvisor (Huang et al., 2020)—and fine-grained expert-level offloading—e.g., MoE-Infinity (Xue et al., 2024), Brainstorm (Cui et al., 2023), Mixtral-Offloading (Eliseev and Mazur, 2023). (iii) Designs utilizing CPU cores for sharing partial computation from GPUs, such as computing less input-intensive experts on CPUs—e.g., Fiddler (Kamahori et al., 2024).

Heterogeneous resources in MoE systems. The sparse nature of MoE models has led system designers to increasingly utilize heterogeneous resources for hosting sparse experts, thus enhancing the cost–performance ratio of these systems. These resources are typically more cost-effective than their GPU counterparts, while still offering significant computing power and memory bandwidth, sufficient for certain operations in MoE models. These resources include: (i) Heterogeneous compute resources, such as CPUs integrated within GPUs (e.g., Grace-Hopper ARM chips) and external CPUs (e.g., AMD and Intel x86 chips). (ii) Heterogeneous memory resources, including LPDDR and HBM in a Grace-Hopper Superchip, DRAM in host CPU, and high-speed SSDs). (iii) Heterogeneous communication resources, featuring chip-to-chip links for HBM-DRAM within GPUs, PCIe for external GPU communications, and NVLink for inter-GPU communication.

Strong demands for evaluating system performance, system cost, and model accuracy. Given the complexity and high cost of deploying MoE systems, users frequently need to assess these systems comprehensively to determine the most cost-effective model and resource configuration. This evaluation typically involves benchmarks that provide metrics reflecting: (i) system performance, including token latency and throughput; (ii) system cost, such as cost per token and energy efficiency (tokens per watt); and (iii) model accuracy, encompassing a variety of metrics such as downstream task accuracy, language modeling perplexity, or hallucination rates.

Often, metrics for cost, performance, and accuracy present conflicting goals, making it challenging to optimize MoE systems across all three dimensions simultaneously. For example, memory offloading often preserves high model accuracy and reduces system costs, but at the expense of system performance. On the other hand, quantization could boost system performance and lower costs but potentially degrade model accuracy. Finally, scaling memory out or up yields more accurate and performant systems but is obviously expensive.

2.1 Limitations of existing benchmarking methods

Many LLM benchmarks have been proposed over the past few years, including MLPerf (Reddi et al., 2020), ML-Energy (You et al., 2023), Open-LLM-Leaderboard (Beeching et al., 2023), LLMPerf (Ilyas Moutawwakil, 2023), TensorDock (TensorDock, 2024), and Artificial Analysis (Artificial Analysis, 2024). To evaluate LLM systems, these benchmarks primarily use three types of metrics: (i) overall system performance metrics, such as token throughput, prefilling time, and decoding time, (ii) cost metrics, like tokens-per-dollar and tokens-per-kilowatt, focusing solely on GPU usage, and (iii) fine-grained system performance metrics, such as MBU and MFU, to facilitate the understanding of memory and compute bottlenecks, as discussed in recent MoE articles (Agarwal et al., 2023). However, when these benchmarks are applied to MoE systems, they demonstrate several limitations.

(1) Lack of principles to understand the relation between cost, accuracy and performance in MoE systems. While MoE systems often claim advantages in cost, accuracy, and performance, their real-world deployment frequently reveals significant challenges. Practitioners often find that deployment costs are underestimated, promised performance benefits over dense alternatives are not achieved, and model accuracy is often compromised. There is a growing need for clear principles to help users effectively assess and understand the complex interplay between these factors.

(2) Inaccurate system performance assessment metrics. A primary limitation is that the MBU and MFU metrics, as currently defined, do not consider selective activation within the sparse MoE layers, leading to an overestimation of memory and compute costs by assuming all model parameters are active (detailed in Section 4). This often leads MoE system operators to substantially over-provision GPUs, causing a significant waste of resources.

(3) Incomplete cost model for entire MoE systems. Additionally, a fallacy of these benchmarks stems from an incomplete analysis of costs in an MoE system. As MoE systems increasingly use heterogeneous resources: hence, relying only on GPU cost data makes existing benchmarks unable to account for the costs associated with additional compute, memory, and communication resources that supplement GPUs, resulting in unreliable cost estimation.

3 The CAP Benchmarking Method for MoE Systems

We propose the following **CAP benchmarking method** for understanding, benchmarking, and comparing MoE systems. The CAP method encompasses three key system optimization metrics:

- **Cost (C):** The deployment cost of an MoE system includes the cost of acquiring all compute and memory hardware required to operate the system, as well as the energy needed to power these resources. For example, the cost of an MoE system that utilizes CPU-assisted computing and parameter offloading to host memory must account for both the CPU and host memory costs.
- **Accuracy (A):** Model accuracy in an MoE system is broadly defined and includes metrics used in widely recognized LLM leaderboards, such as the Open LLM Leaderboard (Beeching et al., 2023), which reflect real-world applications of LLMs.
- **Performance (P):** Performance is assessed through user-facing metrics, such as first-token latency, inter-token latency, and token throughput, as well as internal system metrics like memory bandwidth utilization and computational resource utilization (e.g., FLOPS).

The CAP method (illustrated in Figure 1 Left) argues that **MoE systems can achieve only two of these three metrics**. This trade-off is fundamentally linked to the router-based, sparse architecture of MoE models and the current hardware capabilities.

3.1 Understanding existing MoE systems using the CAP

In the following section, we survey existing MoE systems through our CAP method.

MoE systems for Performance and Accuracy (PA). Improving performance without compromising accuracy can be achieved through two primary approaches: (i) scaling up device memory capacity by utilizing high-end GPUs with large memory (e.g., H200 NVL with 141 GB and MI300X with 192 GB), and (ii) scaling out memory capacity via parallel and distributed computing, leveraging technologies such as NVLinks, NVSwitch, and InfiniBand, along with techniques like Tensor, Pipeline, and Expert parallelism (Li et al., 2023a, Holmes et al., 2024, Li et al., 2023b, Kwon et al., 2023, NVIDIA, 2023). However, these approaches face significant drawbacks: the exponential increase in system costs due to the growing manufacturing complexity of high-speed memory devices and the sub-linear scaling efficiency of distributed systems, where communication increasingly becomes a bottleneck at larger scales.

MoE systems for Performance and Cost (PC). To enhance system performance without increasing costs, MoE models can adopt (i) quantization as low as 8bit (Dettmers et al., 2022, Yi et al., 2023), 4bit (Frantar et al., 2022, Lin et al., 2023, Tang et al., 2024) or even 1bit (Ma et al., 2024) or (ii) compression, such as model distillation (Hsieh et al., 2023) and sparsification (Ansell et al., 2024, Nawrot et al., 2024, Zhong et al., 2024). These methods reduce computational and memory demands but lead to inevitable performance degradation, particularly in terms of accuracy.

MoE systems for Cost and Accuracy (CA). In constrained hardware environments, some systems aim to maintain model accuracy within a limited budget (e.g., relying on low-end GPUs or a restricted number of GPUs). Techniques such as memory swapping (Xue et al., 2024, Cao et al., 2024) are employed to offload model parameters or KV caches based on sparsity. Additionally, some systems utilize CPUs to assist GPU operations during model inference or generation (Kamahori et al., 2024). These systems however, still introduce performance degradation.

3.2 Examples of comparing MoE systems using CAP

The CAP trade-off method offers a robust framework for evaluating the strengths and weaknesses of MoE systems, particularly when they claim to excel in cost, performance, and accuracy. For example, a memory-swapping MoE system (falling under the CA category) and a distributed MoE system (falling under the PA category) both claim cost savings through high performance. However, the CAP framework enables users to clearly identify that the memory-swapping system will have lower performance compared to the distributed alternative.

4 Sparsity-Aware Performance Metrics

In this section, we begin by introducing MBU and MFU and explore the implications of using these metrics to analyze MoE systems. Subsequently, we introduce the Sparse MBU and Sparse MFU, discussing the benchmarking use cases that these new metrics enable.

4.1 Implications of using vanilla MBU and MFU in assessing MoE systems

MBU (Agarwal et al., 2023) and MFU (Chowdhery et al., 2023) are common metrics for assessing the performance of an LLM system. Specifically, the dominating factors affecting the performance can vary with different batch sizes. In scenarios involving small batch sizes, the latency of a generation iteration—measured as time-per-output-token (TPOT)—is primarily influenced by the time required to transfer model parameters from HBM to the SRAM in GPUs. This scenario is characterized as memory-bound, which can be captured by MBU. Conversely, with larger batch sizes, the TPOT is dominated by the time needed by the GPU to complete the computation, making this scenario compute-bound, which can be quantified by MFU.

Implication of MBU. MBU measures the ratio of achieved memory bandwidth to the peak bandwidth (*i.e.* maximum bandwidth obtained from the hardware spec), as defined as:

$$\text{MBU} = \frac{B_{\text{achieved}}}{B_{\text{peak}}}, B_{\text{achieved}} = \frac{S_{\text{model}} + S_{\text{KV}}}{\text{TPOT}}, S_{\text{model}} = n_{\text{layer}} \times (S_{\text{attn}} + S_{\text{ff}}), \quad (1)$$

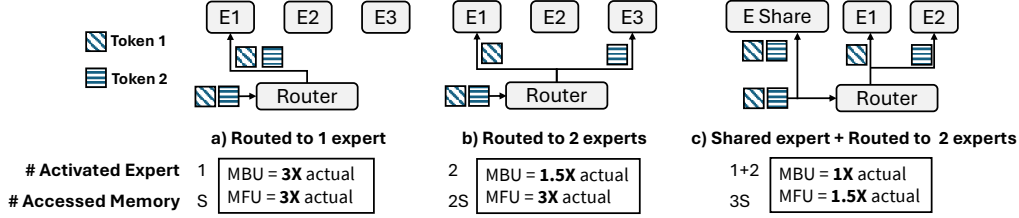


Figure 2: MoE model memory access and performance metrics under three routing scenarios. S represents the size of a single expert. The existing definitions of MBU or MFU include the cost of every expert, without taking routing or expert selection mechanisms into consideration. We indicate how much MBU/MFU is overestimated as a result, compared to the actual MBU/MFU.

where S represents the size of memory access in GB (*e.g.* S_{KV} stands for the KV cache size, S_{model} stands for model size, S_{attn} for attention size, S_{attn} for FFN size) and n_{layer} the number of layers in the model. However, leading MoE practitioners (Agarwal et al., 2023) estimate the achieved memory bandwidth assuming that each generated token goes through all layers and attends to the whole KV cache; hence, the achieved memory bandwidth is proportional to S_{model} and S_{KV} . However, in MoE models, only selected experts (decided by the router) are accessed. For example, in Figure 2 (a), where the router in an MoE layer sends all tokens to one expert, the size of memory access is S . In case (a), MBU given by equation 1 is inflated by up to 3X, resulting in an overestimation of hardware utilization. Similarly, in case (b), two experts are needed while MBU assumes all three, resulting in a $1.5\times$ inflation.

Implication of MFU. MFU is often defined as:

$$\text{MFU} = (T_{\text{token}} \times F_{\text{token}}) / F_{\text{peak}}, \quad (2)$$

where T_{token} is the inference tokens-per-second throughput and F_{token} is the FLOPs per token per forward pass. For dense models excluding self-attention, we have $F_{\text{token}} = 2N$ where N is the total number of parameters. This equation, however, leads to overestimating MFU of MoE models because each token activates top- k experts (and shared experts if any), instead of the entire model. For example, in Figure 2 (a), with one expert participating in computation, MFU is inflated by $3\times$. Also in case (c), each token activates two experts (shared + Top-1), MFU assumes all experts are used, resulting in a $1.5\times$ inflation.

4.2 Sparse Model Bandwidth Utilization

When designing a new sparsity-aware MBU, we want this new metric to be generally applicable to all types of MoE models we are aware of by far. These different sparsity patterns of MoE models can be summarized in Figure 2. From this figure, we can derive several requirements for the new MBU. First, this new metric shall reflect which experts are activated with a batch of input tokens. In case (a), for example, a sparse feed-forward (FF) layer with three experts where each token only activates the top-1 expert. In case (a), the two input tokens activate the same expert after routing (*i.e.* accessed memory is one expert size); while in case (b), two tokens activate two different experts, which doubles the accessed memory compared to (a). Second, the metrics must account for different routing mechanisms, such as shared experts introduced by recent MoE studies (Dai et al., 2024, Bai et al., 2023) (illustrated in Figure 2 (c)).

To meet the above requirements, we define Sparse Memory Bandwidth Utilization (S-MBU) based on the activated size of parameters $S_{\text{activated}}$, rather than using the full model size S_{model} , as follows.

$$\text{S-MBU} = \frac{B_{\text{achieved}}}{B_{\text{peak}}}, \quad B_{\text{achieved}} = \frac{S_{\text{activated}} + S_{KV}}{\text{TPOT}}, \quad S_{\text{activated}} = n_{\text{layer}} \times S_{\text{attn}} + \sum_{l=1}^{n_{\text{layer}}} \sum_{i=1}^{n_{\text{expert}}} \mathbb{1}[l, i] \times S_{\text{expert}}, \quad (3)$$

where $\mathbb{1}[l, i]$ is a boolean variable indicates whether the expert indexed i at layer l is used for computation. This guarantees that only the activated parameters are accounted for the accessed memory for each layer l . $\mathbb{1}[l, i]$ can be achieved by tracing router outputs. Besides, dense models are a special case of equation (3) with $n_{\text{expert}} = 1$ and $\forall i, \mathbb{1}[l, i] = 1$. Therefore, our definition is also suitable for model architectures where not all layers are MoE layers, *e.g.*, in Switch Transformers (Fedus et al., 2022).

4.3 Sparse Model FLOPs Utilization

We aim to account for the fact that experts are sparsely activated when calculating F_{token} , *i.e.* FLOPS per token. Specifically, in each MoE layer, we account for top-k activated experts with shared experts, denoted k_{expert} , which can be obtained from the model configuration without the need for runtime tracing. Besides, we also account for the router component in each MoE layer, N_{router} . The attention layer remains the same. Consequently, we refine the FLOPS per token calculation as follows:

$$\text{S-MFU} = (T_{\text{token}} \times \text{S-}F_{\text{token}}) / F_{\text{peak}}, \quad \text{S-}F_{\text{token}} = 2N_{\text{attn}} + 2N_{\text{router}} + 2k_{\text{expert}}N_{\text{expert}}, \quad (4)$$

where N_{attn} and N_{expert} represent the number of parameters in the self-attention module and the expert module, respectively.

4.4 Practical use cases of S-MBU and S-MFU

S-MBU use cases. After introducing S-MBU as part of our benchmark, we have documented several significant use cases. One notable scenario involves deploying the Mixtral-8x22B model on GPUs using bfloat16 precision, targeting a time-per-output-token (TPOT) of 100ms with a batch size of 1. Practitioners have highlighted several beneficial applications of S-MBU in this context: (i) *Better GPU choice*: Previously, using MBU, an MoE system required a bandwidth of $141\text{B} * 2 \text{ bytes-per-parameter} / 100\text{ms}$, equating to 2.36 TB/s. This MBU-based estimate indicated the necessity to deploy the system on the latest generation H100 GPUs, which offer up to 3.35TB/s with HBM3 technology, thus ruling out the use of less recent, more cost-effective GPUs like the A100 with HBM2, which offers around 2TB/s. After transitioning to S-MBU, the estimated bandwidth requirement has been revised to 0.780 TB/s. This can be met using the A100 and even more cost-effective GPUs like the 4090 (1008 GB/s) and A6000 (768GB/s). (ii) *Better system performance*: While deploying the MoE system on A100, MBU analysis indicates that increasing the batch size further does not enhance efficiency, as the bandwidth is already fully utilized. However, S-MBU analysis suggests that the HBM bandwidth is still underutilized, suggesting an increase of the batch size for improved system performance.

S-MFU use cases. We also report a significant use case for S-MFU in our benchmark. Consider the scenario of serving a DBRX model on GPUs with precision bfloat16, aiming for $T_{\text{token}}=2000$ tokens/s with a batch size of 32. After transitioning to S-MFU, practitioners are more confident in saving the GPUs provisioned for that DBRX model. Previously, MFU estimates indicated that such a batch size would require GPUs capable of delivering at least 500 TFLOPS, achievable only with three A100 GPUs (312 TFLOPS). In contrast, S-MFU offers a more precise estimate of 140 TFLOPS, allowing practitioners to confidently reduce the A100 GPU to one, saving 66% in resources.

5 Complete Cost Model for MoE Systems

In this section, we introduce the design of our cost model, which aims to capture the complexity of managing various heterogeneous resources in an MoE system.

Purchase cost. Upon server decommissioning and during model deployment upgrades, new hardware purchases are factored into the overall cost. From a performance perspective, system choice is influenced by three main components as outlined in Equation 5: computation, communication, and memory capacity. The computation component includes both the GPU and CPU. Communication involves the connectivity within the system, such as the PCIe links between the GPU, CPU, and SSD, and the NVLink connections between GPUs. We also consider the communication between the computation units and memory, specifically CPU-to-DRAM and SRAM-to-HBM in GPUs. Memory is structured in three hierarchical tiers: HBM within the GPU, DRAM as host memory, and SSD storage. More formally, we define Equation 5 as follows where C stands for the dollar cost for the target hardware:

$$\begin{aligned} C_{\text{hardware}} &= \overbrace{(C_{\text{GPU}} + C_{\text{CPU}})}^{\text{computation}} + \overbrace{(C_{\text{C2M}} + C_{\text{PCIe}} + C_{\text{NVLink}})}^{\text{communication}} + \overbrace{(C_{\text{HBM}} + C_{\text{DRAM}} + C_{\text{SSD}})}^{\text{memory}}, \quad (5) \\ &= C_{\text{GPU}} + C_{\text{CPU}} + C_{\text{Motherboard}} + C_{\text{DRAM}} + C_{\text{SSD}}, \end{aligned}$$

Specially, C_{C2M} is the accelerator internal bandwidth cost. Choosing the GPU variant C_{GPU} involves the options for HBM size C_{HBM} , communication links C_{NVLink} and C_{C2M} . Choosing the motherboard variant $C_{Motherboard}$ covers the PCIe cost. Choosing the CPU variant also caps the C_{C2M} .

Energy cost. After the server is purchased and the model is deployed, the primary cost comes from using the hardware, which is reflected as energy consumption. (shown in Equation 6). The energy consumption primarily stems from using the data on the device (computation) and moving the data (communication) between and within devices. The maintenance power draw on each layer of memory is included as the basis for computation and communication. We account for the average power draw over the server runtime R .

$$C_{\text{energy}} = \left[\overbrace{(P_{\text{GPU}} + P_{\text{CPU}})}^{\text{computation}} + \overbrace{(P_{\text{C2M}} + P_{\text{PCIe}} + P_{\text{NVLink}})}^{\text{communication}} \right] \times R \quad (6)$$

Cost-performance. The performance metric (e.g., tokens-per-second throughput) only measures whether the model achieves a guaranteed performance on a given server setting. However, cost efficiency has yet to be considered: how to identify the best server setup to achieve the desired performance? Cost efficiency must take into account both the purchase cost and the energy cost of the model deployment.

$$C_{\text{token}} = (C_{\text{hardware}} + C_{\text{energy}} \times \$/\text{kWh}) / (T_{\text{token}} \times R), \quad (7)$$

We apply Equation (7) to combine both cost models and performance metrics. We aim to determine the per-token cost in units of dollars, denoted as C_{token} . The energy cost in kWh needs to be combined with the local energy price to estimate the cost, as it can vary between industrial/personal energy usage and by region (U.S. Bureau of Labor Statistics, 2024). The C_{token} is calculated over the lifetime R of the deployment and averaged across all generated tokens.

Practical use cases. We have considered several use cases after introducing new cost models as part of our benchmark. For instance, in GPU-only deployments, the specifications for DRAM, CPU, and SSD are typically not defined. Cloud providers often scale the computational power in line with GPU capabilities, offering four times the DRAM capacity (e.g., 2TB DDR5) relative to GPU memory (e.g., 8XA100-80GB), and pair it with the latest CPUs (e.g., AMD 9004 series). This hardware combination results in an approximate cost of \$176,000 per server. Opting for a less powerful CPU and reduced memory capacity in GPU-only workloads can yield a saving of \$20,000 per server in hardware costs.

Additionally, for MoE systems that enable offloading, it is crucial to account for the CPU’s energy consumption and the energy used in communication between the CPU and GPU. For instance, the AMD 777X has a peak consumption of 280W, while the A6000 Ada peaks at 300W. Relying solely on GPU energy assessments might lead to overly optimistic forecasts for energy savings, as the CPU’s power consumption can be as significant as another GPU.

6 MoE-CAP Implementation

In this section, we discuss the implementation of our benchmarking software and discuss the choice of supported datasets and models.

Implementation details. Following the design principle of a Leaderboard on HuggingFace, we implemented MoE-CAP as a leaderboard that showcases different MoE systems’ cost, accuracy, and performance. We made the process of downloading datasets and models and triggering MoE-CAP for evaluation fully automatic. We also made the benchmarking platform extensible, reducing the cost of adding a new MoE system to be considered. The entire benchmark is compatible with HuggingFace software, making it easy to use it as a library (e.g., importing the S-MBU and S-MFU metrics for assessing a custom MoE system). So far, we have included four popular MoE-supported LLM inference frameworks, namely vLLM, TensorRT-LLM, HuggingFace Transformers, and HuggingFace Accelerate. We plan to include more frameworks, such as Ollama and DeepSpeed.

Further, we plan to evaluate MoE deployment cost in varied cloud environments, such as those involving serverless model endpoints (Fu et al., 2024), elastic resources (Wagenländer et al., 2024,

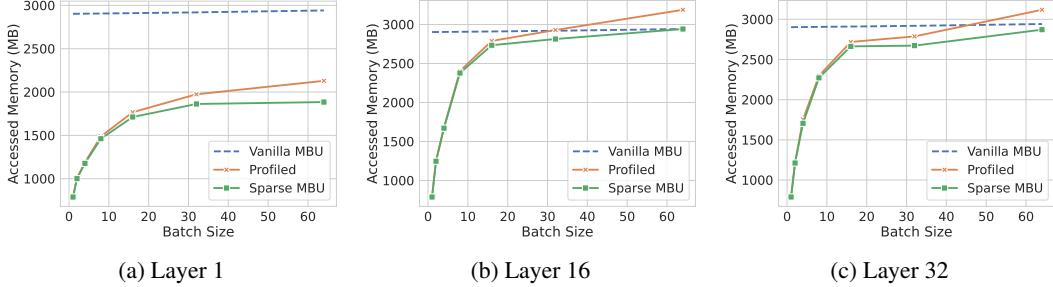


Figure 3: Correctness evaluation of the vanilla MBU, our S-MBU and actual MBU (through profiling).

Wang et al., 2023, Mai et al., 2020), and spot instances (Mao et al., 2024, Miao et al., 2024, Wagenlander et al., 2020)

Models. We evaluate four models: Mixtral-8x7B-Instruct-v0.1, Mixtral-8x22B-Instruct-v0.1, DBRX-instruct, and Qwen1.5-MoE-A2.7-Chat. We chose these MoE models because they are different in either the parameter sizes or the model architecture; in addition, they are known for their strong performance and are commonly recognized and used in both academic and industrial fields. **Mixtral 8x7B** and **Mixtral 8x22B** are MoE language models, each featuring eight experts per layer. At each layer, two experts are selected for each token. **DBRX** extends the number of experts to 16 in each MoE layer and chooses top-4 experts for each token. **Qwen1.5-MoE-A2.7B** features a distinctly different architecture from the previously mentioned models. Apart from top 4 selected experts, it incorporates four shared experts that process each input token. We measure instruction-fine-tuned versions of these four models, which have shown enhanced performance in addressing real-world problems and conversational scenarios.

Datasets. We evaluate them on three distinct datasets: MMLU (Hendrycks et al., 2021), GSM8k (Cobbe et al., 2021), and Arena-Hard (Li et al., 2024). (i) The MMLU dataset assesses MoE LLMs through multiple-choice questions across 57 varied tasks, from basic mathematics to law, ensuring that MoE LLMs develop consistent and reliable factuality and reasoning capabilities across diverse areas. (ii) **Arena-Hard**, which demands long text generation, includes 500 complex user queries from Chatbot Arena and uses GPT4-Turbo (OpenAI et al., 2024) for evaluations instead of humans. Results from Arena-Hard show significantly better separability than other benchmarks, with tighter confidence intervals, and align closely with human preference rankings, demonstrating an agreement rate of 89.1% according to Chatbot Arena evaluations (Zheng et al., 2023). (iii) We also utilize the **GSM8K** dataset, which includes 8,500 grade school math problems requiring multi-step mathematical reasoning and short-form generation.

These three benchmarks examine MoE LLMs’ abilities in multiple-choice, short-form, and long-form generation, challenging their skills in text generation, math, reasoning, and broad knowledge. Overall, they reflect the quality and accuracy of MoE LLMs across a broad range of tasks. Moreover, these benchmarks are widely used in existing leaderboards (Beeching et al., 2023, Ilyas Moutawwakil, 2023, Hong et al., 2024) to rank models based on their test results.

7 Metric Evaluation and Benchmark Results

This section evaluates our proposed metrics and the CAP method. First, we show that S-MBU more accurately reflects actual profiled accessed memory than vanilla MBU. Next, we verify CAP as a practical method for assessing MoE systems. Finally, we use CAP to analyze trade-offs among PC, PA, and CA system configurations.

S-MBU Evaluation. We verify the proposed S-MBU with Mixtral-8x7B model. As discussed in §4.2, vanilla MBU is not aware of the sparse memory access. In Figure 3, we show the averaged accessed memory of a specific Transformer layer of Mixtral-8x7B model using the GSM8K dataset. We vary the input batch size from 1 to 64. With a batch size of 1, in each layer, only the top 2 experts are accessed (*i.e.* activated); instead, with increased batch sizes, more experts are accessed. However, the number of total activated experts does not necessarily increase linearly with batch size because tokens can share experts.

Table 2: Representative benchmarking results for Mixtral-8x22B under PA, CP, and CA configurations.

Framework	vLLM	TensorRT-LLM	MoE-Infinity
Case	PA	CP	CA
Precision	bf16	int4	bf16
# GPU	4	4	2
batch size	32	40	32
Cost (k USD)	92.1	92.1	50.6
Accuracy(%)	82.6	72.6	82.6
Performance (token/s)	104.0	593.4	3.25

Table 3: Trade-offs between throughput and accuracy under fixed cost configurations.

Model	Precision	GSM8K			ArenaHard		
		Accuracy	Cost	Throughput	Accuracy	Cost	Throughput
Mixtral-8x7B	bf16	64.37	92.10	966.00	20.61	92.10	1117.49
	int8	63.08	92.10	1129.15	17.33	92.10	1544.68
	int4	46.85	92.10	1225.00	12.33	92.10	2184.96
Mixtral-8x22B	bf16	82.64	92.10	139.08	32.98	92.10	503.01
	int8	81.58	92.10	308.05	27.86	92.10	703.40
	int4	72.93	92.10	593.42	24.88	92.10	780.23
DBRX	bf16	71.87	92.10	135.18	14.69	92.10	583.64
	int8	70.74	92.10	274.05	11.39	92.10	646.85
	int4	46.10	92.10	335.95	7.17	92.10	752.54

According to Figure 3, the vanilla MBU fails to account for the selective activation of experts in an MoE layer, resulting in an overestimation of total accessed memory by over 260%. In contrast, S-MBU captures the activated experts accurately, with less than a 1% discrepancy from the actual memory usage profiled (based on HuggingFace Transformers). As batch size increases, we observe varying expert activation patterns across layers. For instance, with a batch size of 64, only about half of the experts are activated in the first layer, while in deeper layers like 16 and 32, nearly all experts are activated. The sparse estimation also accurately reflects the trend of increasing memory access with larger batch sizes. However, there remains a gap between the profiled results and both MBU and S-MBU when almost all experts are activated, primarily because both methods overlook the intermediate states (e.g., hidden states) that increase linearly with batch size.

7.1 Benchmarking MoE systems with the CAP method

We first construct and analyze three representative MoE system configurations, each optimized for a distinct pair among PA, CP, and CA. Subsequently, we vary their configurations and examine how shifting design choices affects the trade-offs among cost, accuracy, and performance.

MoE systems achieving PA, CP, and CA. We illustrate three representative MoE configurations using the Mixtral-8x22B model on A100 80GB GPUs, each optimizing a distinct CAP dimension pair. For accuracy-focused (A) cases, we employ bf16 precision; for others, we use int4 quantization. Performance-oriented setups use 4 GPUs for higher FLOPS and bandwidth, while cost-focused configurations use 2 GPUs and offloading. Costs follow the model from §5 and accuracy is measured on GSM8K.

PA (Performance & Accuracy): Using vLLM with bf16 and a batch size of 32 on 4 GPUs, we achieve 104 tokens/s without accuracy loss.

CP (Cost & Performance): TensorRT-LLM with int4 quantization runs at a larger batch size (because quantized model parameters occupy less GPU memory), delivering 593 tokens/s (5.7× improvement) at reduced per-token cost, but drops accuracy by 12%.

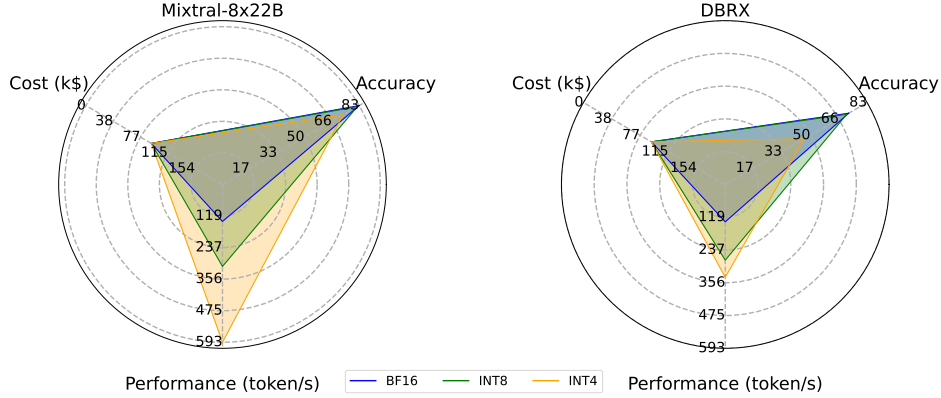


Figure 4: Comparison of CA and CP configurations for Mixtral-8x22B and DBRX on GSM8K in CAP space.

Table 4: Trade-offs between throughput and cost at fixed accuracy configurations.

Model	#GPUs	GSM8K			ArenaHard		
		Accuracy	Cost	Throughput	Accuracy	Cost	Throughput
Mixtral-8x7B	2	64.37	50.64	146.76	20.61	50.64	92.46
	4	64.37	92.10	222.62	20.61	92.10	128.84
	8	64.37	175.03	223.71	20.61	175.03	149.97
Qwen1.5-MoE-A2.7B	1	47.69	29.91	276.21	5.64	29.91	223.83
	2	47.69	50.64	364.62	5.64	50.64	239.74
	4	47.69	92.10	446.16	5.64	92.10	280.60

CA (Cost & Accuracy): MoE-infinity offloads parameters to host memory and uses only 2 GPUs, cutting costs by $1.8\times$ without accuracy loss, but throughput falls drastically to 3.52 tokens/s.

These results confirm that no single configuration attains all three CAP goals simultaneously.

Trading inference accuracy for higher performance (CA vs CP). We now compare inference configurations under equal cost while varying model precision between bf16, int8, and int4 using TensorRT-LLM on 4xA100 80GB GPUs for both Mixtral and DBRX models. Quantization can boost throughput by up to $2.5\times$ at the same cost but sacrifices accuracy, especially on challenging tasks like ArenaHard. For example, Mixtral-8x7B’s accuracy falls from 17.33% to 12.33% from int8 to int4, and DBRX from 14.69% to 7.17%.

The performance gains from quantization differ across models and tasks. Mixtral-8x22B shows a $4\times$ performance increase from bf16 to int4 with only a 12% accuracy drop, making int8 or int4 viable for simpler tasks. Conversely, DBRX exhibits a steeper accuracy loss, making int4 less attractive.

Figure 4 visualizes cost, accuracy, and performance for Mixtral-8x22B and DBRX. Int8 is often the optimal choice if moderate accuracy drops are acceptable, whereas int4 may compromise accuracy too severely in certain models. Overall, quantization must be carefully tuned to strike the right balance between CA and CP.

Trading cost for higher performance (PA vs. AC). Here, we maintain accuracy (no quantization) while varying the number of GPUs for tensor parallelism. For Mixtral-8x7B, we tested 2, 4, and 8 GPUs; for Qwen1.5-MoE-A2.7B, we tested 1, 2, and 4 GPUs. Adding more GPUs increases throughput by up to $1.6\times$ but inflates cost linearly. For instance, expanding from 4 to 8 GPUs for Mixtral-8x7B only improves throughput by $1.16\times$ while nearly doubling cost. These diminishing returns illustrate that scaling GPUs merely for performance is often inefficient.

Figure 5 shows CAP radar charts for these configurations. Increasing GPU counts rapidly inflates cost without proportionate performance gains. While small GPU increments may be justified, large-scale up-scaling tensor parallelism degree provides limited benefit and compromises cost-effectiveness.

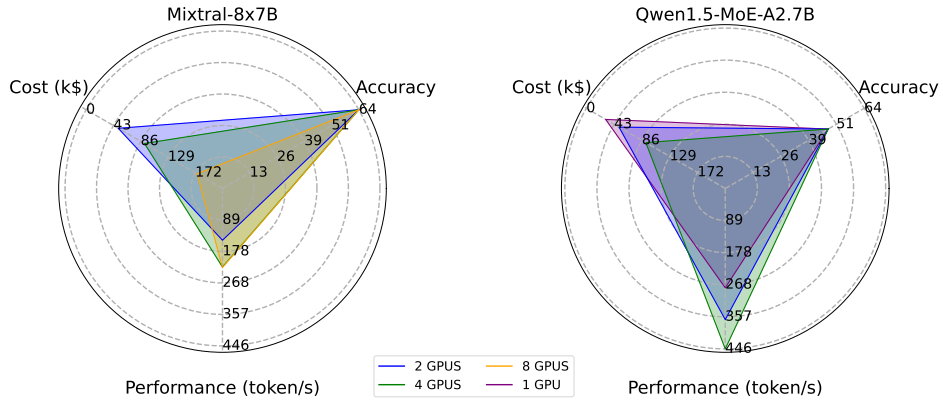


Figure 5: Comparison of PA and AC configurations on GSM8K in CAP space.

In summary, these experiments confirm that CAP trade-offs are intrinsic to MoE systems. By applying CAP, practitioners can visualize potential configurations and select the most suitable deployment strategy—be it PA, AC, or PC—based on their specific requirements. Achieving all three CAP metrics simultaneously remains infeasible with current hardware and models.

8 Conclusion

This paper introduces MoE-CAP, a novel and timely benchmark designed to understand and evaluate emerging MoE systems. We anticipate that the new sparsity-aware performance metrics and the new heterogeneous-resource-aware cost model will be crucial for accurately comparing MoE systems. These metrics are also effective in validating the claims of these systems, particularly when considering the conflicting dimensions of system optimization: performance, cost, and quality.

References

- M. Agarwal, A. Qureshi, N. Sardana, L. Li, J. Quevedo, and D. Khudia. <https://www.databricks.com/blog/llm-inference-performance-engineering-best-practices>, 2023.
- R. Y. Aminabadi, S. Rajbhandari, A. A. Awan, C. Li, D. Li, E. Zheng, O. Ruwase, S. Smith, M. Zhang, J. Rasley, and Y. He. DeepSpeed-Inference: Enabling efficient inference of transformer models at unprecedented scale. In *SC*, pages 46:1–46:15. IEEE, 2022.
- A. Ansell, I. Vulić, H. Sterz, A. Korhonen, and E. M. Ponti. Scaling sparse fine-tuning to large language models, 2024. URL <https://arxiv.org/abs/2401.16405>.
- Artificial Analysis. Artificial analysis llm performance leaderboard. <https://artificialanalysis.ai/leaderboards/models>, 2024. Accessed: 2024-06-04.
- J. Bai, S. Bai, Y. Chu, Z. Cui, K. Dang, X. Deng, Y. Fan, W. Ge, Y. Han, F. Huang, B. Hui, L. Ji, M. Li, J. Lin, R. Lin, D. Liu, G. Liu, C. Lu, K. Lu, J. Ma, R. Men, X. Ren, X. Ren, C. Tan, S. Tan, J. Tu, P. Wang, S. Wang, W. Wang, S. Wu, B. Xu, J. Xu, A. Yang, H. Yang, J. Yang, S. Yang, Y. Yao, B. Yu, H. Yuan, Z. Yuan, J. Zhang, X. Zhang, Y. Zhang, Z. Zhang, C. Zhou, J. Zhou, X. Zhou, and T. Zhu. Qwen technical report. *arXiv preprint arXiv:2309.16609*, 2023.
- E. Beeching, C. Fourrier, N. Habib, S. Han, N. Lambert, N. Rajani, O. Sanseviero, L. Tunstall, and T. Wolf. Open llm leaderboard. https://huggingface.co/spaces/HuggingFaceH4/open_llm_leaderboard, 2023.
- S. Cao, S. Liu, T. Griggs, P. Schafhalter, X. Liu, Y. Sheng, J. E. Gonzalez, M. Zaharia, and I. Stoica. Moe-lightning: High-throughput moe inference on memory-constrained gpu. *arXiv preprint arXiv:2411.11217*, 2024.
- A. Chowdhery, S. Narang, J. Devlin, M. Bosma, G. Mishra, A. Roberts, P. Barham, H. W. Chung, C. Sutton, S. Gehrmann, P. Schuh, K. Shi, S. Tsvyashchenko, J. Maynez, A. Rao, P. Barnes, Y. Tay, N. Shazeer, V. Prabhakaran, E. Reif, N. Du, B. Hutchinson, R. Pope, J. Bradbury, J. Austin, M. Isard, G. Gur-Ari, P. Yin, T. Duke, A. Levskaya, S. Ghemawat, S. Dev, H. Michalewski, X. Garcia, V. Misra, K. Robinson, L. Fedus, D. Zhou, D. Ippolito, D. Luan, H. Lim, B. Zoph, A. Spiridonov, R. Sepassi, D. Dohan, S. Agrawal, M. Omernick, A. M. Dai, T. S. Pillai, M. Pellat, A. Lewkowycz, E. Moreira, R. Child, O. Polozov, K. Lee, Z. Zhou, X. Wang, B. Saeta, M. Diaz, O. Firat, M. Catasta, J. Wei, K. Meier-Hellstern, D. Eck, J. Dean, S. Petrov, and N. Fiedel. PaLM: Scaling language modeling with pathways. *J. Mach. Learn. Res.*, 24:240:1–240:113, 2023.
- K. Cobbe, V. Kosaraju, M. Bavarian, M. Chen, H. Jun, L. Kaiser, M. Plappert, J. Tworek, J. Hilton, R. Nakano, C. Hesse, and J. Schulman. Training verifiers to solve math word problems, 2021.
- W. Cui, Z. Han, L. Ouyang, Y. Wang, N. Zheng, L. Ma, Y. Yang, F. Yang, J. Xue, L. Qiu, L. Zhou, Q. Chen, H. Tan, and M. Guo. Optimizing dynamic neural networks with Brainstorm. In *OSDI*, pages 797–815. USENIX Association, 2023.
- D. Dai, C. Deng, C. Zhao, R. X. Xu, H. Gao, D. Chen, J. Li, W. Zeng, X. Yu, Y. Wu, Z. Xie, Y. K. Li, P. Huang, F. Luo, C. Ruan, Z. Sui, and W. Liang. Deepseekmoe: Towards ultimate expert specialization in mixture-of-experts language models, 2024.
- T. Dettmers, M. Lewis, Y. Belkada, and L. Zettlemoyer. Gpt3. int8 (): 8-bit matrix multiplication for transformers at scale. *Advances in Neural Information Processing Systems*, 35:30318–30332, 2022.
- A. Eliseev and D. Mazur. Fast inference of mixture-of-experts language models with offloading, 2023.
- W. Fedus, B. Zoph, and N. Shazeer. Switch Transformers: Scaling to trillion parameter models with simple and efficient sparsity. *J. Mach. Learn. Res.*, 23:120:1–120:39, 2022.
- E. Frantar and D. Alistarh. Qmoe: Practical sub-1-bit compression of trillion-parameter models, 2023.

- E. Frantar, S. Ashkboos, T. Hoefler, and D. Alistarh. GPTQ: accurate post-training quantization for generative pre-trained transformers, 2022.
- Y. Fu, L. Xue, Y. Huang, A.-O. Brabete, D. Ustiugov, Y. Patel, and L. Mai. Serverlessllm: Low-latency serverless inference for large language models. In *18th USENIX Symposium on Operating Systems Design and Implementation*, pages 135–153. USENIX Association, 2024.
- D. Hendrycks, C. Burns, S. Basart, A. Zou, M. Mazeika, D. Song, and J. Steinhardt. Measuring massive multitask language understanding, 2021.
- C. Holmes, M. Tanaka, M. Wyatt, A. A. Awan, J. Rasley, S. Rajbhandari, R. Y. Aminabadi, H. Qin, A. Bakhtiari, L. Kurilenko, and Y. He. DeepSpeed-FastGen: High-throughput text generation for LLMs via MII and DeepSpeed-Inference, 2024.
- G. Hong, A. P. Gema, R. Saxena, X. Du, P. Nie, Y. Zhao, L. Perez-Beltrachini, M. Ryabinin, X. He, C. Fourrier, and P. Minervini. The hallucinations leaderboard - an open effort to measure hallucinations in large language models. *CoRR*, abs/2404.05904, 2024. doi: 10.48550/ARXIV.2404.05904. URL <https://doi.org/10.48550/arXiv.2404.05904>.
- C.-Y. Hsieh, C.-L. Li, C.-K. Yeh, H. Nakhost, Y. Fujii, A. Ratner, R. Krishna, C.-Y. Lee, and T. Pfister. Distilling step-by-step! outperforming larger language models with less training data and smaller model sizes. *arXiv preprint arXiv:2305.02301*, 2023.
- C. Huang, G. Jin, and J. Li. SwapAdvisor: Pushing deep learning beyond the GPU memory limit via smart swapping. In *ASPLOS*, pages 1341–1355. ACM, 2020.
- R. P. Ilyas Moutawwakil. Llm-perf leaderboard. <https://huggingface.co/spaces/optimum/llm-perf-leaderboard>, 2023.
- A. Q. Jiang, A. Sablayrolles, A. Roux, A. Mensch, B. Savary, C. Bamford, D. S. Chaplot, D. de Las Casas, E. B. Hanna, F. Bressand, G. Lengyel, G. Bour, G. Lample, L. R. Lavaud, L. Saulnier, M. Lachaux, P. Stock, S. Subramanian, S. Yang, S. Antoniak, T. L. Scao, T. Gervet, T. Lavril, T. Wang, T. Lacroix, and W. E. Sayed. Mixtral of experts, 2024.
- K. Kamahori, Y. Gu, K. Zhu, and B. Kasikci. Fiddler: CPU-GPU orchestration for fast inference of mixture-of-experts models, 2024.
- Y. J. Kim, R. Fahim, and H. H. Awadalla. Mixture of quantized experts (MoQE): Complementary effect of low-bit quantization and robustness, 2023.
- W. Kwon, Z. Li, S. Zhuang, Y. Sheng, L. Zheng, C. H. Yu, J. Gonzalez, H. Zhang, and I. Stoica. Efficient memory management for large language model serving with pagedattention. In *SOSP*, pages 611–626. ACM, 2023.
- J. Li, Y. Jiang, Y. Zhu, C. Wang, and H. Xu. Accelerating distributed MoE training and inference with Lina. In *USENIX Annual Technical Conference*, pages 945–959. USENIX Association, 2023a.
- T. Li, W.-L. Chiang, E. Frick, L. Dunlap, B. Zhu, J. E. Gonzalez, and I. Stoica. From live data to high-quality benchmarks: The arena-hard pipeline, April 2024. URL <https://lmsys.org/blog/2024-04-19-arena-hard/>.
- Z. Li, L. Zheng, Y. Zhong, V. Liu, Y. Sheng, X. Jin, Y. Huang, Z. Chen, H. Zhang, J. E. Gonzalez, and I. Stoica. AlpaServe: Statistical multiplexing with model parallelism for deep learning serving. In *OSDI*, pages 663–679. USENIX Association, 2023b.
- J. Lin, J. Tang, H. Tang, S. Yang, X. Dang, and S. Han. AWQ: activation-aware weight quantization for LLM compression and acceleration, 2023.
- S. Ma, H. Wang, L. Ma, L. Wang, W. Wang, S. Huang, L. Dong, R. Wang, J. Xue, and F. Wei. The era of 1-bit llms: All large language models are in 1.58 bits. *arXiv preprint arXiv:2402.17764*, 2024.
- L. Mai, G. Li, M. Wagenländer, K. Fertakis, A.-O. Brabete, and P. Pietzuch. {KungFu}: Making training in distributed machine learning adaptive. In *14th USENIX Symposium on Operating Systems Design and Implementation (OSDI 20)*, pages 937–954, 2020.

- Z. Mao, T. Xia, Z. Wu, W.-L. Chiang, T. Griggs, R. Bhardwaj, Z. Yang, S. Shenker, and I. Stoica. Skyserve: Serving ai models across regions and clouds with spot instances. *arXiv preprint arXiv:2411.01438*, 2024.
- X. Miao, C. Shi, J. Duan, X. Xi, D. Lin, B. Cui, and Z. Jia. Spotservice: Serving generative large language models on preemptible instances. In *Proceedings of the 29th ACM International Conference on Architectural Support for Programming Languages and Operating Systems, Volume 2*, pages 1112–1127, 2024.
- P. Nawrot, A. Łańcucki, M. Chochowski, D. Tarjan, and E. M. Ponti. Dynamic memory compression: Retrofitting llms for accelerated inference, 2024. URL <https://arxiv.org/abs/2403.09636>.
- NVIDIA. TensorRT-LLM. <https://github.com/NVIDIA/TensorRT-LLM>, 2023.
- OpenAI, J. Achiam, S. Adler, S. Agarwal, L. Ahmad, I. Akkaya, F. L. Aleman, D. Almeida, J. Al-tenschmidt, S. Altman, S. Anadkat, R. Avila, I. Babuschkin, S. Balaji, V. Balcom, P. Baltescu, H. Bao, M. Bavarian, J. Belgum, I. Bello, J. Berdine, G. Bernadett-Shapiro, C. Berner, L. Bogdonoff, O. Boiko, M. Boyd, A.-L. Brakman, G. Brockman, T. Brooks, et al. Gpt-4 technical report, 2024.
- V. J. Reddi, C. Cheng, D. Kanter, P. Mattson, G. Schmuelling, C.-J. Wu, B. Anderson, M. Breughe, M. Charlebois, W. Chou, R. Chukka, C. Coleman, S. Davis, P. Deng, G. Diamos, J. Duke, D. Fick, J. S. Gardner, I. Hubara, S. Idgunji, T. B. Jablin, J. Jiao, T. S. John, P. Kanwar, D. Lee, J. Liao, A. Lokhmotov, F. Massa, P. Meng, P. Micikevicius, C. Osborne, G. Pekhimenko, A. T. R. Rajan, D. Sequeira, A. Sirasao, F. Sun, H. Tang, M. Thomson, F. Wei, E. Wu, L. Xu, K. Yamada, B. Yu, G. Yuan, A. Zhong, P. Zhang, and Y. Zhou. Mlperf inference benchmark. In *2020 ACM/IEEE 47th Annual International Symposium on Computer Architecture (ISCA)*, pages 446–459, 2020. doi: 10.1109/ISCA45697.2020.00045.
- Snowflake AI Research. Snowflake Arctic: The best LLM for enterprise AI — efficiently intelligent, truly open. <https://www.snowflake.com/blog/arctic-open-efficient-foundation-language-models-snowflake/>, 2024. Accessed: 2024-06-04.
- P. Tang, J. Liu, X. Hou, Y. Pu, J. Wang, P.-A. Heng, C. Li, and M. Guo. Hobbit: A mixed precision expert offloading system for fast moe inference, 2024.
- TensorDock. Tensordock - machine learning gpu benchmarks. <https://tensordock.com/benchmarks>, 2024. Accessed: 2024-06-04.
- M. I. O. U.S. Bureau of Labor Statistics. Average energy prices for the united states, regions, census divisions, and selected metropolitan areas. https://www.bls.gov/regions/midwest/data/averageenergyprices_selectedareas_table.htm, 2024. Accessed: 2024-06-04.
- M. Wagenländer, L. Mai, G. Li, and P. Pietzuch. Spotnik: Designing distributed machine learning for transient cloud resources. In *12th USENIX Workshop on Hot Topics in Cloud Computing (HotCloud 20)*, 2020.
- M. Wagenländer, G. Li, B. Zhao, L. Mai, and P. Pietzuch. Tenplex: Dynamic parallelism for deep learning using parallelizable tensor collections. In *Proceedings of the ACM SIGOPS 30th Symposium on Operating Systems Principles*, pages 195–210, 2024.
- Z. Wang, Z. Jia, S. Zheng, Z. Zhang, X. Fu, T. E. Ng, and Y. Wang. Gemini: Fast failure recovery in distributed training with in-memory checkpoints. In *Proceedings of the 29th Symposium on Operating Systems Principles*, pages 364–381, 2023.
- XAI. Open release of Grok-1. <https://x.ai/blog/grok-os>, 2024. Accessed: 2024-06-04.
- G. Xiao, J. Lin, M. Seznec, H. Wu, J. Demouth, and S. Han. SmoothQuant: Accurate and efficient post-training quantization for large language models. In *ICML*, volume 202 of *Proceedings of Machine Learning Research*, pages 38087–38099. PMLR, 2023.
- L. Xue, Y. Fu, Z. Lu, L. Mai, and M. Marina. Moe-infinity: Activation-aware expert offloading for efficient moe serving, 2024.

- R. Yi, L. Guo, S. Wei, A. Zhou, S. Wang, and M. Xu. EdgeMoE: Fast on-device inference of moe-based large language models, 2023.
- J. You, J.-W. Chung, and M. Chowdhury. Zeus: Understanding and optimizing GPU energy consumption of DNN training. In *USENIX NSDI*, 2023.
- L. Zheng, W.-L. Chiang, Y. Sheng, S. Zhuang, Z. Wu, Y. Zhuang, Z. Lin, Z. Li, D. Li, E. Xing, H. Zhang, J. E. Gonzalez, and I. Stoica. Judging llm-as-a-judge with mt-bench and chatbot arena. In *Thirty-seventh Conference on Neural Information Processing Systems Datasets and Benchmarks Track*, 2023. URL <https://openreview.net/forum?id=ucCHPGDlao>.
- S. Zhong, L. Liang, Y. Wang, R. Wang, R. Huang, and M. Li. AdapMoE: Adaptive sensitivity-based expert gating and management for efficient moe inference, 2024.